DISTRIBUTION STATEMENT A. Approved for public release; distribution is unlimited.

Light Scattering by Marine Particles: Modeling with Non-spherical Shapes

Howard R. Gordon
Department of Physics
University of Miami
Coral Gables, FL 33124
Phone: (305) 284-2323-1, Fax: (305) 284-4222, email: hgordon@miami.edu

Grant Number N000140710226

LONG-TERM GOALS

The long-term scientific goal of my research is to better understand the distribution of phytoplankton in the world's oceans through remote sensing their influence on the optical properties of the water. An associated goal is the understanding of the absorption and backscattering properties of marine particles in terms of the distributions of their size, shape, and composition.

OBJECTIVES

The inherent optical properties (IOPs) of marine particles are most-often modeled as homogeneous spheres using Mie Theory. Although this approach has been fruitful, the next logical step in modeling marine particles is to abandon the normally-employed spherical approximation and use more realistic approximations to their shape. The advent of computer codes capable of handling more complex shapes, and the increased computational speeds now available, suggest that particle modeling employing simple non-spherical shapes, e.g., disks, rods, etc., could become routine. For example, Gordon and Du (2001) used a two-disk model to try to reproduce the backscattering by coccoliths detached from *E. huxleyi* in the blue-green region of the spectrum. They found that the gross morphology of the particle (e.g., modeling the coccolith as parallel disks as opposed to a single disk of the same diameter and volume) was paramount in determining the spectral variation of backscattering. Later Gordon et al. (2009) showed that the resulting spectral variation of the backscattering cross section for the two-disk model agreed with experiment, and that additional fine structure evident in SEM images of coccoliths had only a minor influence on the backscattering. In another study, Clavano et al. (2007) looked at the IOP of spheroids (ellipses of revolution) as a function of their size and aspect ratio (larger major axis divided by smaller major axis) using refractive indices in the range found for marine particles. Their results suggest that, when compared to equal volume spheres, shape can be a significant factor in the IOPs, especially backscattering.

The work described here represents the culmination of my research into computation of the IOPs of non-spherical objects. Of particular interest to me was the scattering and absorption of particles showing significant deviation from spheres, e.g., cylinders with large aspect ratios. This gross morphology resembles long chain phytoplankton. My objective was to provide answers to the following questions. How do their scattering and absorption properties depend on the length, diameter and index of refraction of the cylinders, or more significantly, their aspect ratio (AR = length ÷

diameter)? Do their IOPs reach a limit in which they become simply proportional to the cylinder's length, so their length-normalized IOPs become independent of aspect ratio? How do they depend on the distribution of absorbing pigments within the cylinder? How do they depend on orientation? How do they compare to the scattering and absorption by spheres containing the same volume of material and quantity of absorbing pigment? Is the spherical approximation effective in interpreting their scattering and absorption in terms of an equivalent refractive index? My goal was to develop an understanding at a level that would allow the incorporation of shape information into IOP models and in the analysis of IOP data.

APPROACH

Of the several computer codes that allow accurate computation of the scattering and absorption properties of individual particles with smooth nonspherical shapes, I employed the discrete-dipole approximation (DDA, Draine, 1988; Draine and Flatau, 1994), as I had used it earlier in my study of particles similar to *E. huxleyi* coccoliths. For the later parts of the study I used an improved version of the code (DDSCAT 7.0). I examined randomly oriented finite cylinders with length up to 25 μm and diameters up to 1.5 μm. At this size, an equal volume sphere has a diameter of about 4 μm.

WORK COMPLETED

I have completed a study of the scattering and backscattering of non-absorbing randomly-oriented cylinders (diameter of 0.5-1.5 μm) as a function of the length and the index of refraction (1.02 to 1.20). The goal was to understand at what aspect ratio the backscattering becomes essentially proportional to the length. This was mostly carried out using the DDSCAT 6.1 code. For the study of absorbing particles, I have modified the new DDSCAT 7.0 code to include cylinders with internal structure, i.e., a coated cylinder. This structure was chosen to represent a long chain of phytoplankton, e.g., diatoms, in which the absorbing pigment, if any, is packaged within the internal cylinder.

I considered absorbing cylinders ranging in diameter from 0.5 to 1.5 μm and lengths from 0.5 to 15 μm. Two sets of cylinders that I examined were homogeneous and had refractive indices $1.05–0.002i$ and $1.05–0.010i$. Two other sets were coated cylinders in which the inner cylinder had a diameter equal to half the cylinder diameter and indices of $1.05–0.008i$ and $1.05–0.040i$. The outer cladding had an index of 1.05 (no absorption). The cylinder with homogeneous index of $1.05–0.010i$ and the coated cylinder with core index $1.05–0.040i$ have exactly the same quantity (mass or number of molecules) of absorbing pigment.

The quantities that I computed were the orientationally-averaged extinction cross section, σ_c, the scattering and backscattering cross sections, σ_b and σ_{bb}, the absorption cross section, σ_a, and the scattering phase function (differential scattering cross section divided by σ_b). The extinction and absorption efficiencies, Q_c and Q_a, are the associated cross sections divided by the orientationally averaged projected area of the particle (the area of the particle's shadow formed by the incident beam, $LD/2$).

The final report of this work was submitted to ONR April 15, 2011.

RESULTS

The main finding of the study was that for $AR > \sim 3\text{-}5$, Q_c and Q_a, become independent of AR and, in fact, close to those computed for infinite cylinders. Similar results are obtained for the scattering phase function and the backscattering probability (σ_{bb}/σ_b).

Figure 1 provides the computed values of Q_c and Q_a for the all aspect ratios examined with absorbing cylinders ($m_i > 0$) and $m_r = 1.05$. The notation in the legend is provided in the figure caption. The upper two panels are for all aspect ratios (1/3 – 30) and the lower panels for $AR \geq 3$. The lines correspond to exact computations for infinite cylinders with the same diameter computed with the IPHASE code (Evans, 1988; Fournier and Evans, 1996). For the case with weaker absorption, the results clearly show that the efficiencies closely follow those for infinite cylinders as long as $AR \geq 3$, for both the coated and the homogeneous cylinders. For the case with stronger absorption, the so-called "package effect," the decrease in absorption when the absorbing molecules are not uniformly distributed within the particle, results in lower absorption efficiency.

This packaging effect displayed more clearly in Figure 2, for which I provide the ratio of the absorption efficiencies Q_a for a coated cylinder with indices $m_{inside} = 1.05–0.040i$ and $m_{outside}$ $1.05–0.000i$ (Q_a(Packaged)) to that of a homogeneous cylinder $m_{inside} = m_{outside} = 1.05–0.010i$ (Q_a(Homo)). Note that both cylinders contain the same number of absorbing molecules. The figure shows that the effect of the absorbing pigment packaging is greatest in the blue region of the spectrum and for larger-diameter cylinders. The maximum decrease in Q_a due to the packaging is about 25% in this case. Although the symbols do not differentiate between cylinder lengths, for a given diameter the packaging effect is largest in the shortest cylinder and depends very little on the length once AR exceeds unity. In the case with less overall absorption, i.e., $m_{inside} = 1.05–0.008i$ and $m_{outside} =$ $1.05–0.000i$ compared to that of a homogeneous cylinder $m_{inside} = m_{outside} = 1.05–0.002i$, similar results are obtained (not shown); however, the maximum decrease in Q_a due to the packaging is only about 10%.

The extinction efficiencies of finite cylinders with larger values of ρ are compared with those of infinite cylinders in Figure 3. In this case the refractive index is 1.20, and since there is no absorption, $Q_b = Q_c$. The figures clearly show that for $AR \geq 3$, the scattering efficiency is again close to that of an infinite cylinder, with all cases except two differing from an infinite cylinder by less than ±10% (RMS difference ~ 5%).

I have shown that the extinction and absorption efficiencies of micrometer-sized cylindrical particles depend little on the aspect ratios as long as $AR \geq 3$. Is this the case for the phase function and backscattering probability? Figure 4 provides an example of the weak dependence of the scattering phase function (and degree of linear polarization) on aspect ratio. Virtually the only differences in the phase function between $AR = 20$ and $AR = 3$ are the enhanced scattering near zero degrees and the deeper minima near 30°, 50°, 80°, and 130° for $AR = 20$. This weak dependence on aspect ratios as long as $AR \geq 5$ is also displayed by the backscattering probability as shown in Figure 5 for a wide range of refractive indices and particle diameters.

IMPACT/APPLICATIONS

The fact that (normalized) IOPs by cylinders with aspect ratios of 3-5 become independent of the aspect ratio can be used to simplify computation of such for analysis of particle scattering. For example, computation of the scattering efficiencies for infinite cylinders (which can be carried out very efficiently) can be used to estimate the same for cylinders with $AR > 3$ with an error < 5-10%. These efficiencies can then be used to compute the cross sections for the cylinder length of interest. Similarly, the backscattering probability for long cylinders with diameters ~ 1-3 times the wavelength (which cannot be computed with most light scattering codes) can be deduced (within 5-10%) from those of finite cylinders with $AR \sim 3$-5. These observations can simplify the analysis of light scattering and absorption by high-aspect ratio particles.

RELATED PROJECTS

None.

REFERENCES

Calvano, W. R., E. Boss, and L. Karp-Boss, Inherent Optical Properties of Non-spherical Marine-Like Particles – From Theory to Observation., *Oceanography and Marine Biology: An Annual Review*, **45**, 1—38 (2007).

Draine, B.T., The discrete-dipole approximation and its application to interstellar graphite grains. *Astrophys. J.* **333**: 848–872, 1988.

Draine, B.T. and P. Flatau, "Discrete-dipole approximation for scattering calculations," J. *Opt. Soc. Am. A* **ll,** 1491–1499, 1994.

Evans, B.T.N. "An interactive program for estimating extinction and scattering properties of most particulate clouds," MRL Rep. R-1123/88 (Materials Research Laboratory, Melbourne, Australia, 1988).

Fournier G.R. and B.T.N. Evans, Approximations to extinction from randomly oriented circular elliptical cylinders, *Appl. Opt*., **35**, 4271—4282 (1996).

Gordon, H.R. and Tao Du, Light scattering by nonspherical particles: application to coccoliths detached from *Emiliania huxleyi*, *Limnology and Oceanography*, **46**, 1438–1454, 2001.

Gordon, H.R., T.J. Smyth, W.M. Balch, and G.C. Boynton, Light scattering by coccoliths detached from *Emiliania huxleyi*, *Applied Optics*, (2009).

PUBLICATIONS

H.R. Gordon, Light scattering by randomly-oriented cylinders: Dependence on aspect ratio for refractive indices applicable for marine particles, *Optics Express*, **19**, 4673–4691 (2011) [published, refereed]

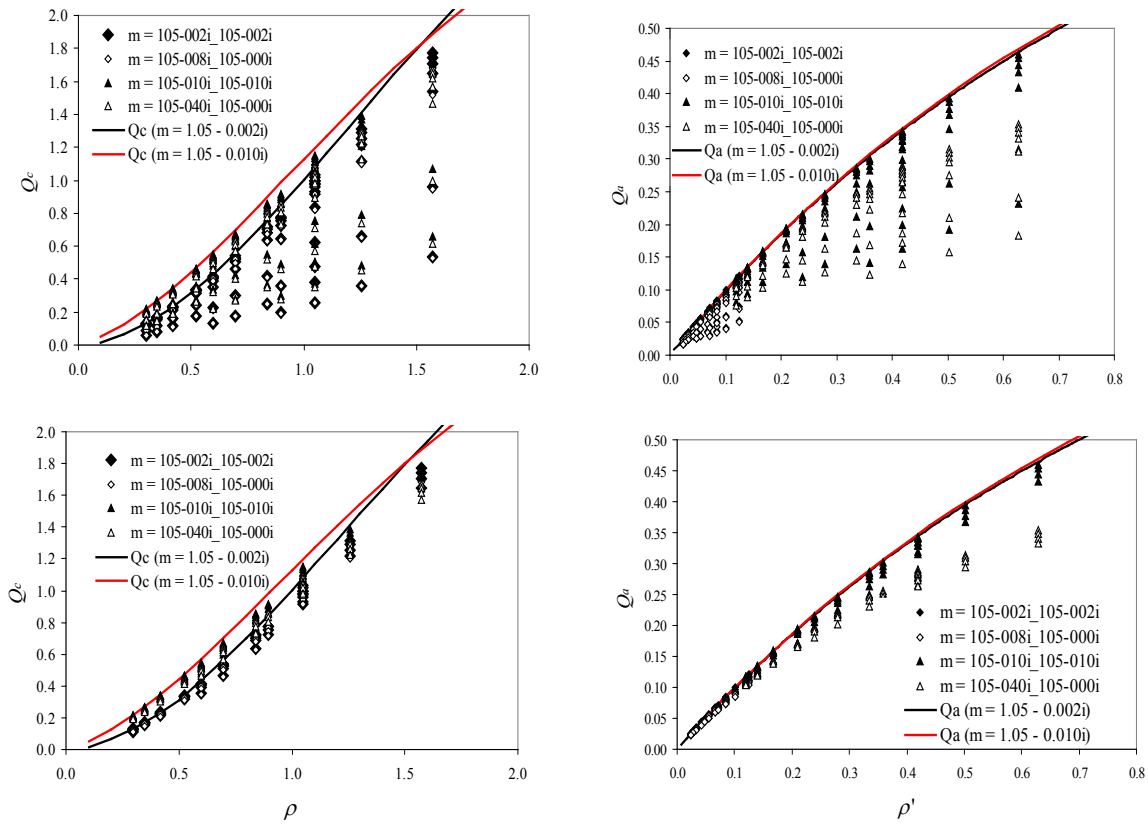

Figure 1. Extinction and absorption efficiencies computed for randomly orientated, homogeneous or coated cylindrically shaped particles, given that their diameter and aspect ratio are known so that their orientationally-averaged projected area is DL/2. Here, $\rho = 2\alpha(m_r - 1)$ and $\rho' = 4\alpha m_i$, where $m_r - im_i$, is the refractive index of the particle relative to water, and $\alpha = \pi D/\lambda$, with D the cylinder's (outer) diameter and λ the wavelength of light in the water. Solid lines are the exact computations for randomly oriented, infinite cylinders. The notation "m=1.05-040i_1.05-000i" indicates that the refractive index of the core is 1.05 – 0.040i, and the refractive index of the coating is 1.05 – 0.000i, etc. In the case of coated cylinders, ρ and ρ' are computed using m_i of the associated homogeneous particle. Top: all aspect ratios (1/3 – 30). Bottom: all aspect ratios ≥ 3. The graphs clearly show that the efficiencies closely follow those for infinite cylinders as long as AR ≥ 3, for both the coated and the homogeneous cylinders. For the case with stronger absorption, the so-called "package effect," the decrease in absorption when the absorbing molecules are not uniformly distributed within the particle, results in lower absorption efficiency.

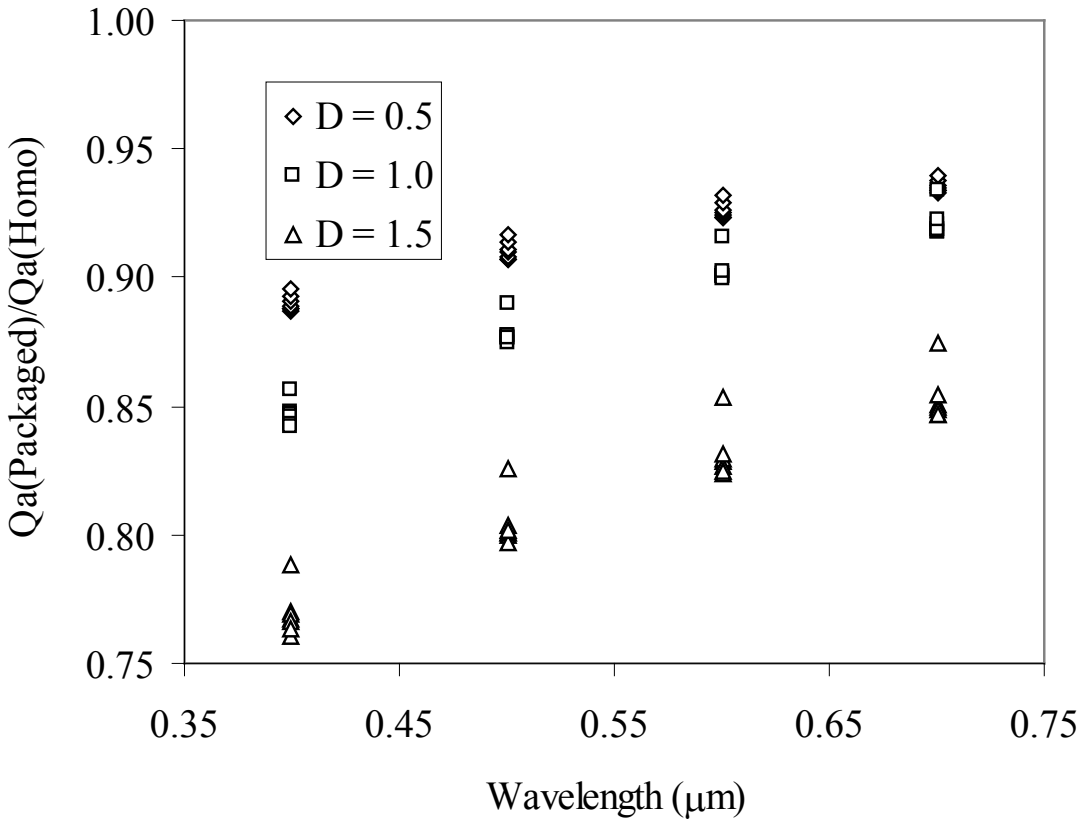

Figure 2. This figure provides the ratio of absorption efficiencies (coated to homogeneous) of the more strongly absorbing cylinders as a function of wavelength. The diameter of the cylinder (in μm) is specified in the legend. For each diameter, the symbols refer to cylinder lengths ranging from 0.5 to 15 μm. The figure shows that the effect of the absorbing pigment packaging is greatest in the blue region of the spectrum and for larger-diameter cylinders. Although the symbols do not differentiate between cylinder lengths, for a given diameter the packaging effect is smallest in the shortest cylinder and depends very little on the length once the aspect ratio (length/diameter) exceeds unity.

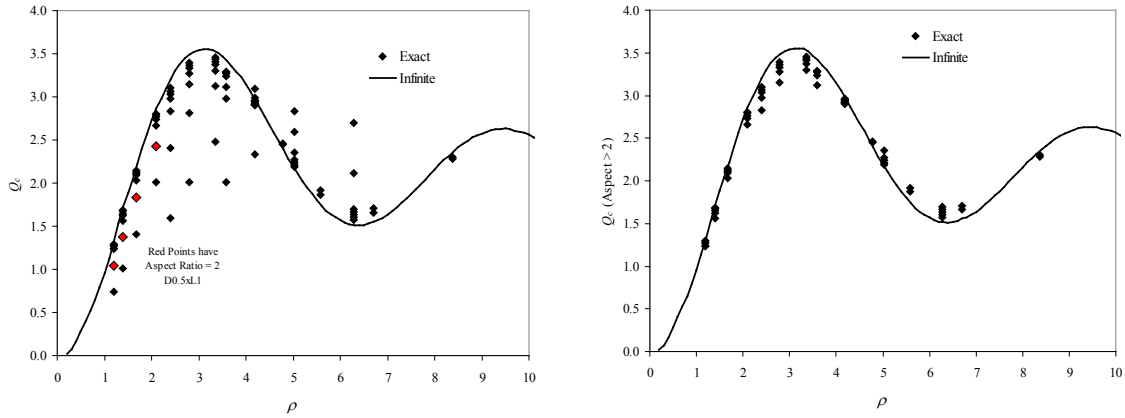

Figure 3. Q_c computed for non-absorbing cylinders (m = 1.20 – 0.000i) with diameters (D) ranging from 0.5 μm to 2.0 μm. Left: 0.25 ≤ AR ≤ 30 (points colored in red are AR = 2). Right: 3 ≤ AR ≤ 30. The solid curve is the extinction efficiency (for a unit length) of randomly-oriented infinite cylinders. As in Figure 1, $\rho = 2\alpha(m - 1)$ with $\alpha = \pi D/\lambda$. The figures clearly show that for AR ≥ 3, the scattering efficiency is again close to that of an infinite cylinder, with all cases except two differing from an infinite cylinder by less than ±10% (RMS difference ~ 5%).

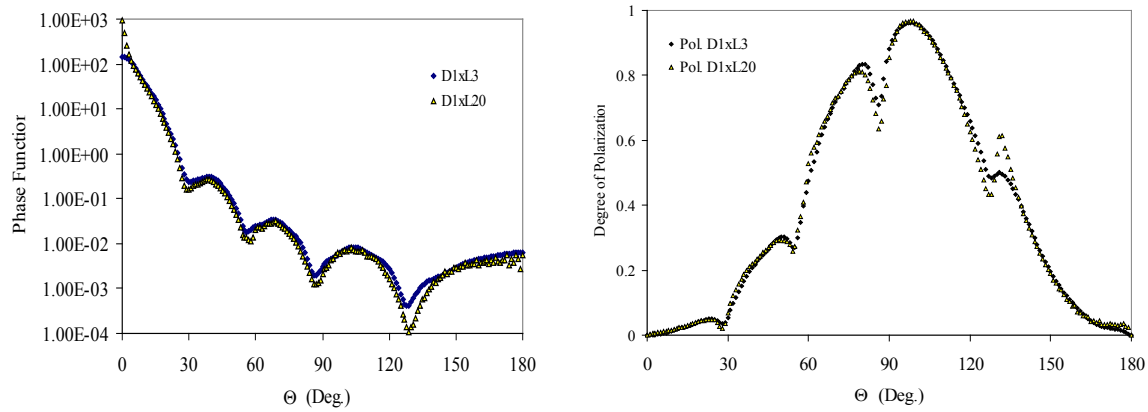

Figure 4. Orientationally-averaged scattering phase functions (left) and degree of polarization (right) at 600 nm (vacuum) for homogeneous cylinders with a diameter of 1 μm and length of 3 μm (D1xL3) and 20 mm (D1xL20). The refractive index is 1.05 – 0.002i. Virtually the only differences in the phase function between AR = 20 and AR = 3 are the enhanced scattering near zero degrees and the deeper minima near 30°, 50°, 80°, and 130° for AR = 20.

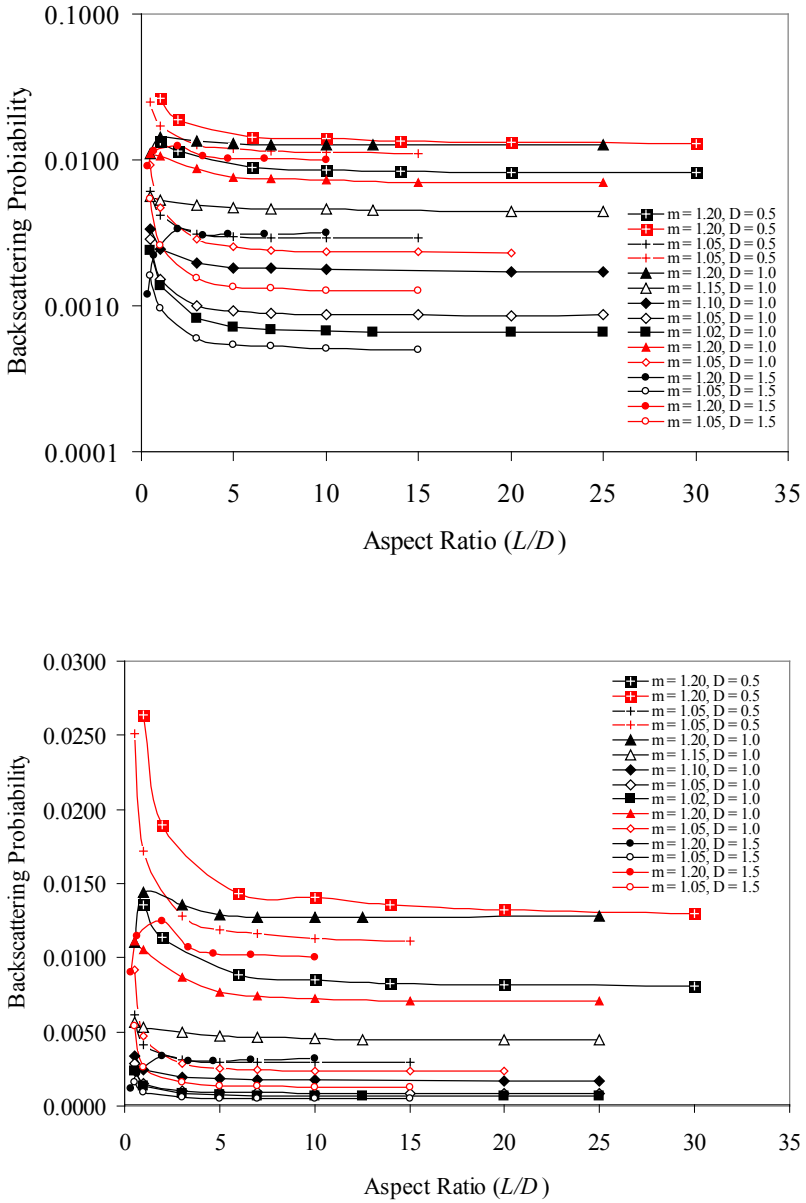

Figure 5. Examples of the variation of the backscattering probability with aspect ratio for cylinder diameters between 0.5 and 1.5 μm and refractive indices ranging from 1.02 to 1.20. The black curves are for a vacuum wavelength of 400 nm and the red curves for 700 nm. The graphs show that there is very little variation in the backscattering probability with aspect ratio for AR > 5.